



Benchmark problems with flexural-torsional coupling for direct analysis method in ANSI/AISC 360-16

Heera M Titus¹, S Arul Jayachandran²

Abstract

The Direct Analysis Method (DAM) of ANSI/AISC 360-16 enables the prediction of design strength in columns without the use of effective length factors. While adopting DAM, a designer must ensure that the software used to calculate the design demands, can capture the second-order effects accurately. For two-dimensional (2D) second-order analysis of steel framed structures, there are several benchmark problems published in the literature, and in contrast very few for 3D frames. This paper presents 3D benchmark problems that accurately capture coupled flexural, and torsional behavior. A geometrically exact total Lagrangian formulation is used where Euler angles define the rigid body dynamics of the system in space. The governing equations in space coordinates are formed using fully nonlinear, objective Jaumann strains and stresses before using principle of virtual work to obtain a 16-degree-of-freedom space beam element. Two benchmark problems are presented - (i) a right angle bent which has no restraint to out-of-plane displacements, and (ii) the bent frame with adequate restraints against out-of-plane displacements at the joints. In the former, the lateral-torsional deformations of the beam cause significant biaxial bending moments in the column. In the second benchmark problem, the behavior of the frame with adequate lateral restraint is brought out. The notional loads have been applied to cause a coupled biaxial bending and twist deformations. It was shown that the exclusion of twist from the deformation response of the frame leads to the underestimation of design demands which is evident from the interactive surface. The paper also suggests a few combinations of notional loads to bring out the true buckling behavior of the frame.

1. Introduction

Direct Analysis Method (DAM) provides a straightforward and transparent tool for the stability analysis and design of steel frames. It requires the judicious use of an advanced analysis tool, which can accurately capture the effect of geometric imperfections and spread of inelasticity in the analysis, whereas the design procedure is exceedingly simplified. DAM avoids the use of effective length factors (K) of a compression member and empirical column curves in determining the axial and flexural capacities of the member (P_n and M_n), and provides a more realistic distribution of second-order forces and bending moments (P_u and M_u). The modifications that are made to the

¹ Research Scholar, Indian Institute of Technology Madras, <heer.titus@gmail.com>

² Professor, Indian Institute of Technology Madras, <aruls@civil.iitm.ac.in>

second-order elastic analysis to include the effect of geometric imperfections, and spread of inelasticity include (Dierlein G 2003; Shankar Nair and Nair 2007; Surovek and Ziemian 2005; Surovek and White 2001):

- (i) The out-of-plumbness is included in the analysis by applying a notional load at each story level given by $N_i = 0.002Y_i$, where Y_i is the factored design gravity load acting on the i^{th} story.
- (ii) The nominal (axial, flexural, and shear) stiffnesses of all the components are factored by 0.8.

For doubly symmetric beam-column members under uniaxial compression and biaxial bending, the interaction shall be limited by (ANSI/AISC 360 2016):

$$\begin{aligned} \frac{P_u}{2\phi P_n} + \frac{M_{ux}}{\phi M_{nx}} + \frac{M_{uy}}{\phi M_{ny}} &\leq 1.0, & \frac{P_u}{\phi P_n} &< 0.2 \\ \frac{P_u}{\phi P_n} + \frac{8}{9} \left(\frac{M_{ux}}{\phi M_{nx}} + \frac{M_{uy}}{\phi M_{ny}} \right) &\leq 1.0, & \frac{P_u}{\phi P_n} &\geq 0.2 \end{aligned} \quad (1)$$

where P_n = available compressive strength, M_{nx} = available flexural strength for major axis flexure, and M_{ny} = available flexural strength for minor axis flexure. In the effective length method (ELM), P_n is determined using effective buckling length (KL) in the plane of bending, whereas, in DAM, P_n is calculated using $K=1$ ($KL=L$) in the plane of bending. While ELM is less sensitive than DAM to the accuracy of the analysis tool used, it requires determining the effective length factor (K), which is difficult for structures with unusual geometries. When compared to ELM, DAM is versatile, reliable, and rational to be implemented in design offices using commercially available softwares.

DAM requires a rigorous second-order analysis tool to determine the design loads acting on frame members. As per AISC-16, the nonlinear analysis method used should accurately capture (i) all axial, flexural, and shear deformations of the members, connection deformations, (ii) second-order effects, (iii) geometric imperfections, (iv) spread of inelasticity, and (v) all uncertainties. Hence, a designer needs to assess the capabilities of the analysis tool in capturing second-order effects, before proceeding to use it in DAM. Benchmark (BM) problems are suggested in the literature to help the designer determine the accuracy and rigor of the software used to determine P_u and M_u . Most of the BM problems available in the literature will have a significant second-order response and will help unveil a particular aspect of structural behavior that could not be ignored or approximated while using DAM. BM problems capturing different structural behaviors including moment frames, braced frames, gable frames, unsymmetric moment frames, unsymmetric braced frames, etc. (Chen and Toma 1994; Du et al. 2019; Ingkiriwang and Far 2018; Surovek and White 2001; Constance W. Ziemian and Ziemian 2021; C. W. Ziemian and Ziemian 2021) are widely available in the literature for use in stability design. A beam element validated using 2D benchmark problems may still be unable to capture the full load-deformation response of a 3D frame, especially twist and out-of-plane deformations. When the frame is made up of torsionally flexible sections (like I sections), as the loading approaches major axis flexural capacity, a small amount of twist itself can create minor axis demands. (Ziemian et al. 2018; Ziemian and Abreu 2018). Traditional design methods account for torsional deformations within the calculation of available strength. In a robust method like DAM, this issue needs to be addressed completely and explicitly in the second-order analysis. 3D space frames exhibiting a system flexural-torsional mode were studied by Du et al. 2019 and Teh 2004.

When imperfections are directly modeled, then the imperfection pattern should be such that it provides the greatest destabilizing effect, and should be similar to displacement under actual external loads and anticipated buckling modes. Instead of directly modeling imperfections, AISC 360-16 suggests the use of lateral notional loads to all types of gravity-loaded frames. Sometimes, a designer may be under the illusion that a 3D analysis is necessary only when the topology of the structure does not permit a 2D analysis. But, this is not true. When a 2D frame is composed of open sections, torsional deformations (or twists), which is an important aspect of frame stability may not be fully revealed when analyzed using a plane frame element. A 3D buckling analysis will identify flexural and flexural-torsional modes. Yet, when the topology and loading are on the same plane, a GNL analysis may still give deformations corresponding to flexural mode, unless an out-of-plane perturbation is applied. This aspect has significant effects on the accuracy of DAM. While limit states involving torsional deformations are a practical reality, even finite element software packages like ABAQUS may not provide out-of-plane torsional deformations when the perfect 2D plane frame with in-plane flexural loads is kept unperturbed. Hence, a single in-plane notional load may not be able to capture the flexural-torsional mode exhibited by the frame. When a 2D frame under in-plane gravity loads has a beam with lateral-torsional buckling as the primary mode of failure, then an in-plane notional load that simulates the sway mode leads to under-estimation of displacement response of the frame. In such cases, an out-of-plane notional load alone can trigger twisting and flexural-torsional deformations of the frame.

This paper describes a geometrically exact 3D finite element (an ongoing work at IIT Madras, India) for the development of benchmark problems for DAM. A simple cantilever L frame under in-plane loading is suggested to highlight the necessity of a spatial analysis even when the frame is planar. The results were validated using a general-purpose finite element software package ABAQUS. It was suggested that while designing any arbitrary frame using DAM, a few combinations of notional loads (as in-plane and out-of-plane individual forces, and as couples), need to be applied to ensure that no particular mode of deformation has been ignored during the analysis.

2. Geometrically exact Total Lagrangian formulation for 3D beam elements- For proposing accurate benchmark problems

Geometrically exact modeling of a 3D beam requires an exact description of the deformed reference line and deformed cross-section. A geometric nonlinear 3D beam element in Total Lagrangian format proposed by Pai (2007; 2000) in the finite displacement-small strain range is described in this section.

2.1 Beam kinematics

A TL method is adopted here with three coordinate systems to define the motion of a beam element. Euler angles are used to define the rigid body dynamics of the system. Consider the initially curved and twisted beam with xyz describing the undeformed state, and $\xi\eta\zeta$ describing the deformed system. abc is a reference coordinate system fixed in space. $i_a, i_b, i_c, i_x, i_y, i_z, i_1, i_2, i_3$ represent the unit vectors along the direction of $a, b, c, x, y, z, \xi, \eta,$ and ζ respectively.

$$\bar{R} = A(s)i_a + B(s)i_b + C(s)i_c \quad (2)$$

$$i_x = \frac{d\bar{R}}{ds} = A'(s)i_a + B'(s)i_b + C'(s)i_c$$

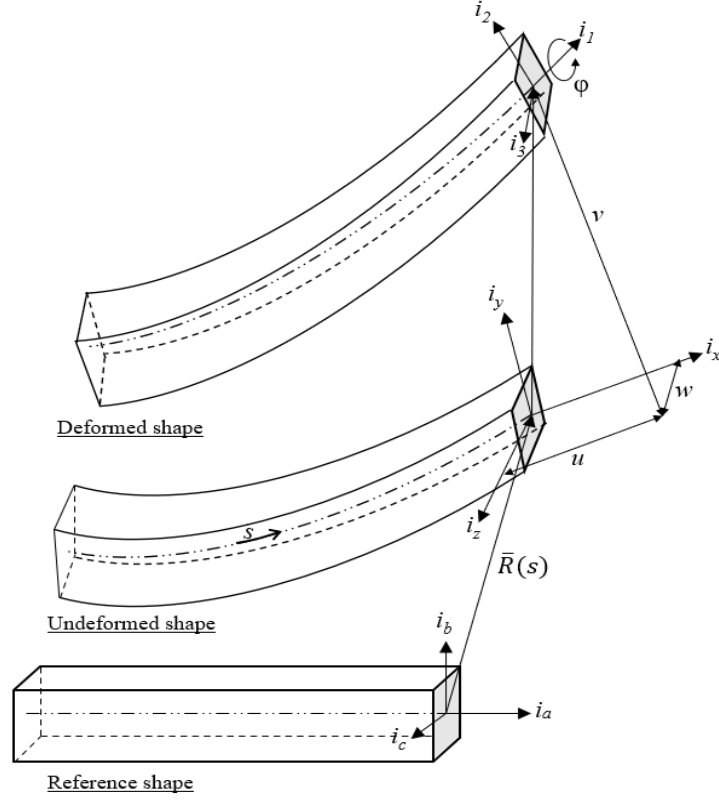


Figure 1: Three coordinate reference systems for modeling

If θ_{21} , θ_{22} , and θ_{23} are the direction cosine angles of the y -axis with respect to abc system, then:

$$\begin{Bmatrix} i_x \\ i_y \\ i_z \end{Bmatrix} = [T^x] \begin{Bmatrix} i_a \\ i_b \\ i_c \end{Bmatrix} \quad (3)$$

$$[T^x] = \begin{bmatrix} A' & B' & C' \\ \cos(\theta_{21}) & \cos(\theta_{22}) & \cos(\theta_{23}) \\ B' \cos(\theta_{23}) - C' \cos(\theta_{22}) & C' \cos(\theta_{21}) - A' \cos(\theta_{23}) & A' \cos(\theta_{22}) - B' \cos(\theta_{21}) \end{bmatrix} \quad (4)$$

As per Frenet-Serret formula,

$$\frac{d}{ds} \begin{Bmatrix} i_x \\ i_y \\ i_z \end{Bmatrix} = [k] \begin{Bmatrix} i_x \\ i_y \\ i_z \end{Bmatrix} = \begin{bmatrix} 0 & k_3 & -k_2 \\ -k_3 & 0 & k_1 \\ k_2 & -k_1 & 0 \end{bmatrix} \begin{Bmatrix} i_x \\ i_y \\ i_z \end{Bmatrix} = \frac{\partial [T^x]}{\partial s} [T^x]^T \begin{Bmatrix} i_x \\ i_y \\ i_z \end{Bmatrix} \quad (5)$$

k_1 , k_2 , and k_3 denote the initial curvatures of the undeformed configuration with respect to the x , y , and z axes, respectively, and are functions of the undeformed arc length s . Similar to the work of Pai (2014), three Euler angles were used to describe the rigid body rotation, thereby giving the formula,

$$\frac{d}{ds} \begin{Bmatrix} i_1 \\ i_2 \\ i_3 \end{Bmatrix} = [K] \begin{Bmatrix} i_1 \\ i_2 \\ i_3 \end{Bmatrix} = \begin{bmatrix} 0 & \rho_3 & -\rho_2 \\ -\rho_3 & 0 & \rho_1 \\ \rho_2 & -\rho_1 & 0 \end{bmatrix} \begin{Bmatrix} i_1 \\ i_2 \\ i_3 \end{Bmatrix} = \frac{\partial [T]}{\partial s} \begin{Bmatrix} i_x \\ i_y \\ i_z \end{Bmatrix} + [T] \frac{d}{ds} \begin{Bmatrix} i_x \\ i_y \\ i_z \end{Bmatrix} \quad (6)$$

$$[K] = [T]' [T]^T + [T][k][T]^T = ([K][T] - [T][k])[T]^T + [T][k][T]^T$$

where the components of the transformation matrix $[T]$ are expressed in terms of $u, v, w, u', v', w', k_1, k_2,$ and k_3 as given below:

$$T_{11} = \frac{(1+u'-vk_3+wk_2)}{(1+e)}, \quad T_{12} = \frac{(v'+uk_3-wk_1)}{(1+e)}, \quad T_{13} = \frac{(w'-uk_2+vk_1)}{(1+e)} \quad (7)$$

$$e = \sqrt{(1+u'-vk_3+wk_2)^2 + (v'+uk_3-wk_1)^2 + (w'-uk_2+vk_1)^2} - 1$$

$$T_{21} = -\cos(\phi)T_{12} - \sin(\phi)T_{13}, \quad T_{22} = \cos(\phi) \left(T_{11} + \frac{T_{13}^2}{1+T_{11}} \right) - \sin(\phi) \left(\frac{T_{12}T_{13}}{1+T_{11}} \right)$$

$$T_{23} = \sin(\phi) \left(T_{11} + \frac{T_{12}^2}{1+T_{11}} \right) - \cos(\phi) \left(\frac{T_{12}T_{13}}{1+T_{11}} \right), \quad T_{31} = \sin(\phi)T_{12} - \cos(\phi)T_{13}$$

$$T_{32} = -\sin(\phi) \left(T_{11} + \frac{T_{13}^2}{1+T_{11}} \right) - \cos(\phi) \left(\frac{T_{12}T_{13}}{1+T_{11}} \right), \quad T_{33} = \cos(\phi) \left(T_{11} + \frac{T_{12}^2}{1+T_{11}} \right) + \sin(\phi) \left(\frac{T_{12}T_{13}}{1+T_{11}} \right)$$

2.2 Variation of kinematic quantities and principle of virtual work

To derive a set of governing equations, describing motion along three perpendicular directions, variations of curvatures in terms of variations of displacements, displacement gradients, and rotations are needed.

$$\begin{Bmatrix} \delta\rho_1 \\ \delta\rho_2 \\ \delta\rho_3 \end{Bmatrix} = \begin{Bmatrix} (\delta\theta_1)' \\ (\delta\theta_2)' \\ (\delta\theta_3)' \end{Bmatrix} - [k] \begin{Bmatrix} \delta\theta_1 \\ \delta\theta_2 \\ \delta\theta_3 \end{Bmatrix} \quad (8)$$

The strain measures used to determine elastic strain energy must contain only strainable displacements. The elastic deformation of the system is calculated by subtracting components of rigid body displacements from total displacement. The strainable displacement vector will consist of relative displacements with respect to the local coordinate system $\xi\eta\zeta$. Using this local displacement field, the fully nonlinear, objective Jaumann strains are:

$$B_{11} = e + z\bar{\rho}_2 - y\bar{\rho}_3, \quad B_{12} = -\frac{1}{2}z\bar{\rho}_1, \quad B_{13} = \frac{1}{2}z\bar{\rho}_1 \quad (9)$$

$$B_{22} = B_{23} = B_{33} = 0, \quad \bar{\rho}_i = \rho_i - k_i$$

where k_i is the initial curvature of the beam. If J_{ij} represents the Jaumann stresses, the total variation of potential energy is:

$$\int_0^L \left(- \left[\left(\{F_1, F_2, F_3\} [T] \right)' + \{F_1, F_2, F_3\} [T] [k] \right] \{ \delta u, \delta v, \delta w \}^T \right) ds + \left[M_1 \delta \theta_1 + M_2 \delta \theta_2 + M_3 \delta \theta_3 + \{F_1, F_2, F_3\} [T] \{ \delta u, \delta v, \delta w \}^T \right]_0^L = 0 \quad (10)$$

where,

$$F_1 = \int_A J_{11} .dA, \quad M_1 = \int_A (J_{13} .y - J_{12} .z) .dA, \quad M_2 = \int_A (J_{11} .z) .dA, \quad M_3 = \int_A (-J_{11} .y) .dA,$$

$$F_2 = \frac{1}{1+e} (-M_3' - M_2 \rho_1 + M_1 \rho_2 - q_6), \quad F_3 = \frac{1}{1+e} (M_2' - M_3 \rho_1 + M_1 \rho_3 + q_5)$$

$q_1, q_2,$ and q_3 are distributed loads along the $x, y,$ and z axes, and $q_4, q_5,$ and q_6 are distributed moments along $\xi, \eta,$ and ζ axes, respectively. From the variational form, the governing equation of motion of a 3D beam element is:

$$[k][T]^T \begin{Bmatrix} F_1 \\ F_2 \\ F_3 \end{Bmatrix} - \frac{\partial}{\partial s} \left([T]^T \begin{Bmatrix} F_1 \\ F_2 \\ F_3 \end{Bmatrix} \right) = \begin{Bmatrix} q_1 \\ q_2 \\ q_3 \end{Bmatrix} \quad (11)$$

2.3 Finite element formulation

For a structure discretized into n_e elements, the variation of strain energy is:

$$\delta \Pi = \{ \delta q \}^T [K] \{ q \} = \sum_{i=1}^{n_e} \{ \delta q^{(i)} \}^T [k^{(i)}] \{ q^{(i)} \} \quad (12)$$

$$\text{where } [k^{(i)}] \{ q^{(i)} \} = \int_{L_i} [\partial N]^T [\Psi]^T [D] \{ \psi \} .ds$$

$$\{ q^{(i)} \} = \left\{ u_j, v_j, w_j, u'_j, v'_j, w'_j, T_{21j}, T_{23j}, u_k, v_k, w_k, u'_k, v'_k, w'_k, T_{21k}, T_{23k} \right\}^T$$

The weak form of the system is given as:

$$\delta \Pi = \int_0^L \{ \delta \psi \}^T [D] \{ \psi \} .ds \quad (13)$$

where

$$[D] = \begin{bmatrix} EA & 0 & 0 & 0 \\ 0 & GI_1 & 0 & 0 \\ 0 & 0 & EI_2 & 0 \\ 0 & 0 & 0 & EI_3 \end{bmatrix}, \{ \psi \} = \{ e, \rho_1 - k_1, \rho_2 - k_2, \rho_3 - k_3 \} \quad (14)$$

$$\{ \delta \psi \} = [\Psi] \{ \delta U \}, \Psi_{ij} = \frac{\partial \psi_i}{\partial U_j}, \{ U \} = [\partial N] \{ q^{(i)} \} = [\partial][N] \{ q^{(i)} \}$$

where $[N]$ is a 5×16 matrix of shape functions of Hermite cubic polynomials and linear polynomials, and $[\partial]$ is a 13×5 matrix of differential operators. The global nodal load vector $\{R\}$ is obtained using:-

$$\delta W = \sum_{i=1}^{n_e} \{\delta q^{(i)}\}^T \{R^{(i)}\} = \{\delta q\}^T \{R\} \quad (15)$$

The equations of motion in matrix form are:

$$[K]\{q\} = \{R\} \quad (16)$$

The above system of nonlinear equations is linearized and solved using arc-length-based solution procedures. The accuracy of the method has been verified against existing benchmark problems in the literature (Pai 2011). Even though DAM needs an accurate nonlinear analysis, using such rigorous methods as described in this section even for the simplest geometries requires modeling and computational effort. Hence, this method is used to generate benchmark problems so that a second-order analysis tool validated using these problems will have enough qualities to assess the nonlinear response of any arbitrary structure for use in DAM.

3. Benchmark problems

3.1 Cantilevered right-angled frame with no lateral restraint

This benchmark problem intends to reveal that when a sway frame is unbraced against out-of-plane deformations:-

- (i) the lateral-torsional deformations of a beam can cause significant biaxial bending moments in the supporting column,
- (ii) and, notional loads should be positioned in such a way that the perfect frame bends in-plane and out-of-plane, and twists under the applied load.

Figure 2 shows a right-angled cantilever frame with in-plane gravity loads at the free end, which primarily fails through lateral-torsional buckling of the beam. δF_x and δF_z represent the fictitious lateral notional loads applied, to perturb the perfect frame in its primary path to the desired secondary path. A geometric nonlinear analysis using a 3D beam element detects torsional deformations only when the imperfection pattern follows the mode shape associated with flexural-torsional buckling of the frame. Otherwise, only in-plane deformations associated with sway will be obtained. Since this is a sway frame under gravity load, if a horizontal notional load alone ($\delta F_x \neq 0$, $\delta F_z = 0$) is applied, the out-of-plane deformations will be zero. To trigger the torsional mode, the notional load applied should be in the z -direction ($\delta F_x = 0$, $\delta F_z \neq 0$). Figure 3 shows the deformed shapes of the frame for a particular load level when subjected to in-plane and out-of-plane notional loads. With a perturbation in the same plane as that of the frame, the frame is too stiff, the in-plane displacements are underpredicted and out-of-plane displacements are zero. When the frame is perturbed in the z -direction, the system is driven into its secondary path, the structure deflects laterally and outward, and deformations are very high in the post-buckled region. To understand how the exclusion of twist from the deformation response leads to the underestimation of design loads, three different models are studied. The applicability of DAM and ELM on the frame is discussed. For ELM, the effective length factor of the column was taken as 2. Three separate analyses are required and the parameters of each model are tabulated in Table 1.

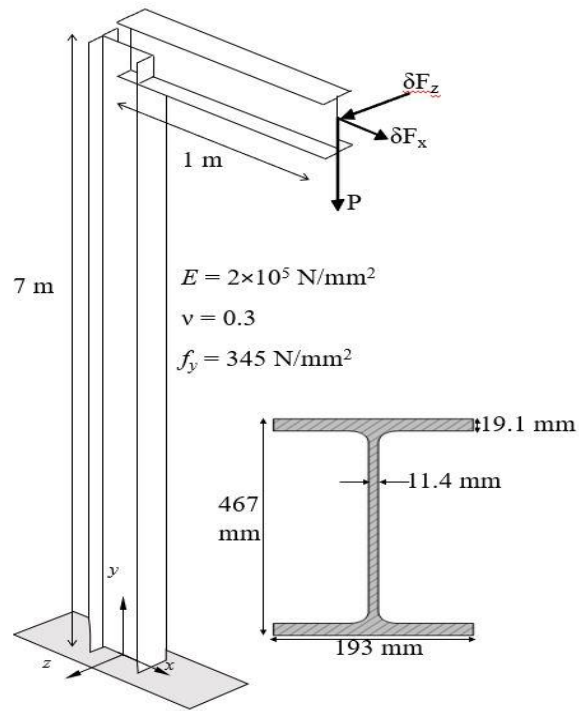


Figure 2: Cantilever right-angled frame

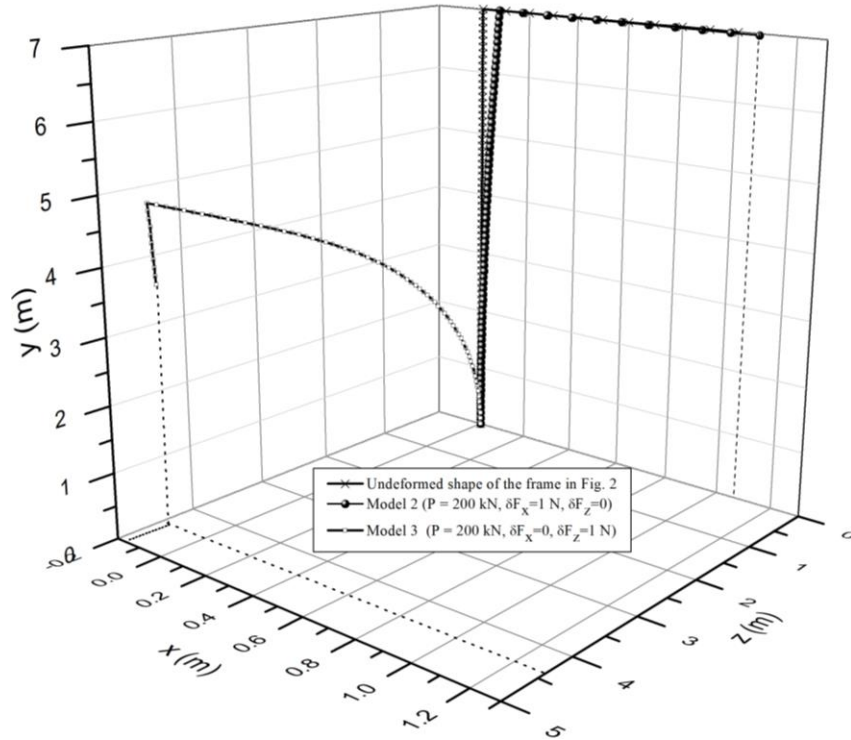


Figure 3: Flexural and flexural-torsional deformations of the frame

Table 1: Modeling parameters for analysis of cantilever frame in Figure 2

| | Parameter | ELM | DAM | |
|--|---|--|---|---|
| | | Model 1 | Model 2 | Model 3 |
| Modeling for nonlinear analysis | Stiffness reduction factor | 1 | 0.8 | 0.8 |
| | Notional loads | No ($\delta F_x=0$, $\delta F_z=0$) | One in-plane notional load ($\delta F_x=1$ N, $\delta F_z=0$) | One out-of-plane notional load ($\delta F_x=0$, $\delta F_z=1$ N) |
| Determination of P_n and M_n (kN and kNm) | Effective length factor (K) | 2 | 1 | 1 |
| | Nominal compressive strength, | 201.4 | 805.5 | 805.5 |
| | Member major axis flexural strength, M_{nx} | 135.7 | 135.7 | 135.7 |
| | Minor axis flexural strength, M_{ny} | 114.5 | 114.5 | 114.5 |
| Determination of P_u and M_{ux} (kN and kNm) | Allowable compressive force, P_u | 86 | 120 | 83.7 |
| | Allowable major axis moment, M_{ux} | 88.1 | 125.2 | 82.6 |

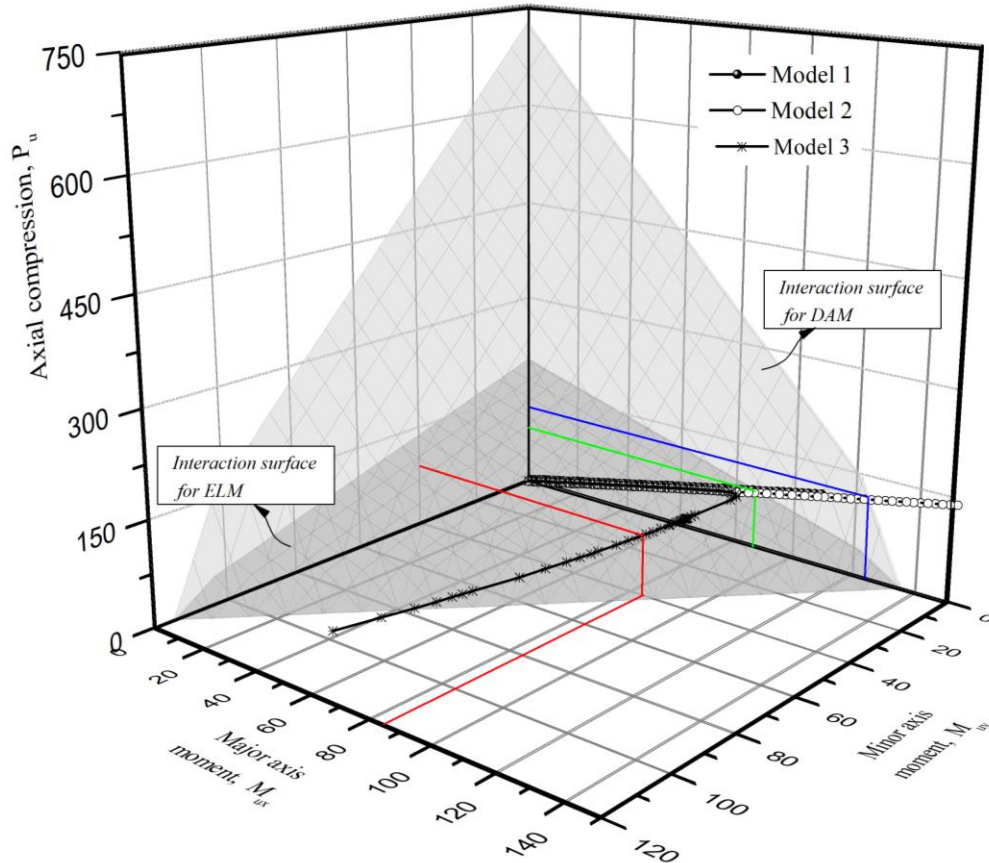


Figure 4: P - M_x - M_y interaction surfaces for ELM and DAM

Figure 4 shows the P - M curves for models 1, 2, and 3, along with the interaction surfaces for ELM ($K=2$) and DAM ($K=1$). For model 1, the P_u - M_{ux} curve represents the true response of the frame under applied loads. The effect of member imperfections and member inelasticity is included in the determination of P_n , M_{nx} , and M_{ny} . As per ELM, the maximum load that can be resisted by the frame is $P=86$ kN. The non-dimensionalized interaction curves and the surface is shown in Figure 5. The attributes of model 2 and model 3 correspond to the DAM requirements. When an in-plane fictitious notional load was applied, the capacities in uniaxial compression and major axis flexure predicted by DAM were much higher than that predicted by ELM. This is because the frame is too stiff under in-plane flexural loading with very high resistance against sway mode, whereas the critical load for the lateral-torsional buckling of the beam is very low. With a notional load acting out-of-plane, the perfect frame is perturbed to a secondary path corresponding to the torsional mode, hence P_u and M_{ux} predicted by Model 3 for DAM are in good agreement with that predicted by ELM.

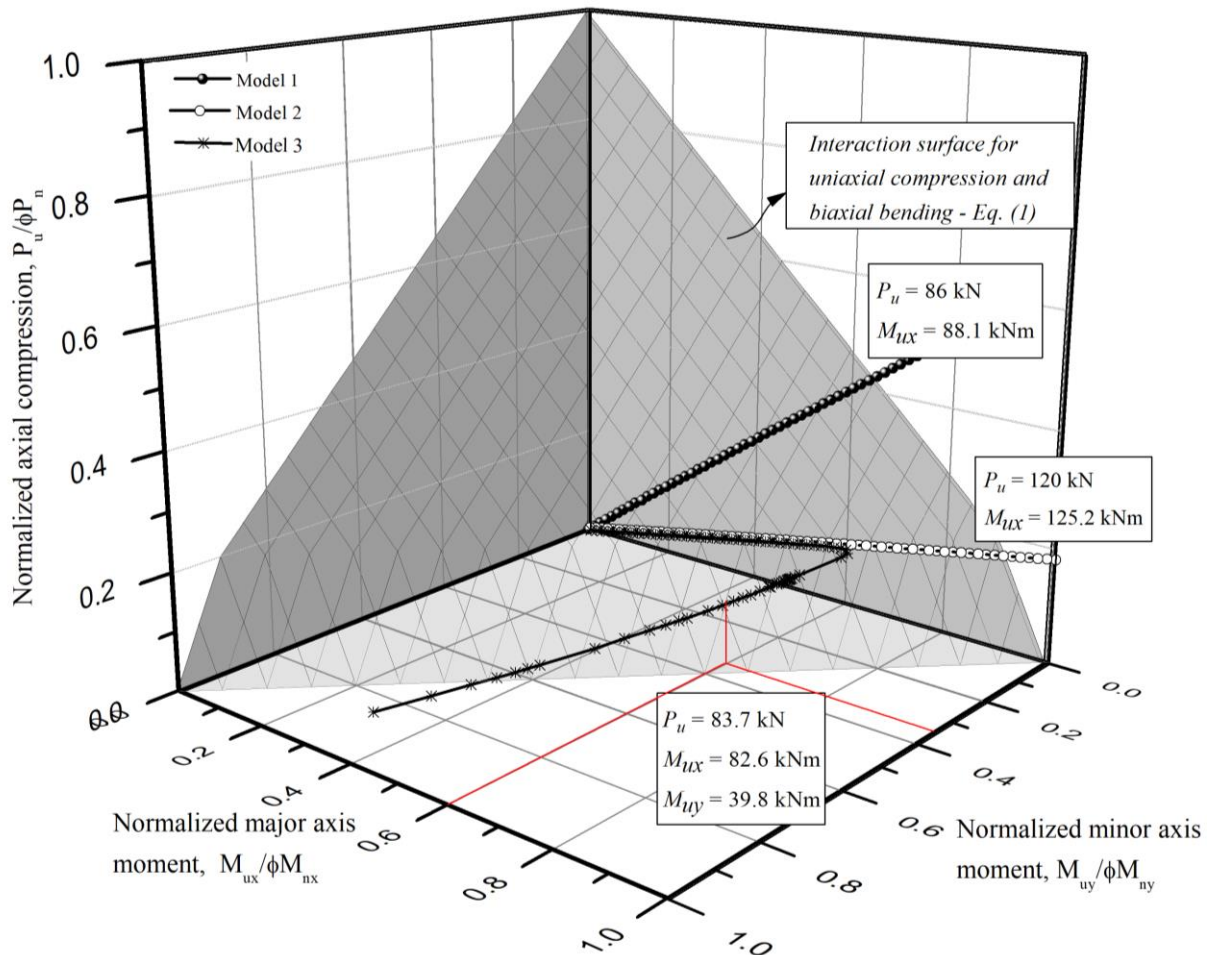


Figure 5: Normalized interaction surface for a member subjected to uniaxial compression and biaxial flexure

If the twisting of the beam and the resulting minor axis moment on the column is unaccounted for in the geometric nonlinear analysis, then DAM will predict member capacities that are higher than the actual capacity of the frame. The design may be unsafe. In this example, the application of an out-of-plane notional load brought out the true response of the frame. Since DAM omits the need

for a buckling analysis, if the designer without understanding the actual response of the structure, assumed that a 3D or 2D frame analysis with in-plane notional loads will suffice for this geometry, then the frame will be too stiff, and the capacities predicted by DAM will be unrealistic. Hence, even when the 2D plane frame is lightly loaded, and the loads are on the same plane as the frame, the designer needs a buckling analysis to identify whether the primary mode of failure is sway or flexural-torsional. But, this takes away the advantage provided by DAM over ELM concerning the determination of the effective length factor. Thus, it is suggested that when the behavior is not clearly understood by the designer, a few combinations of notional loads may be tried by the designer on the frame to reveal the entire spectrum of deformation responses of the structure to the applied loads.

3.2 Cantilevered right-angled frame with adequate lateral restraint at joints

This benchmark problem intends to reveal that when a sway frame is adequately braced against out-of-plane deformations at the joints:-

- (i) the minor axis flexure demand of the column is nominal as the out-of-plane sway of the frame is prevented,
- (ii) and, notional loads should be positioned in such a way that the perfect frame will undergo out-of-plane member deformations if any, under the applied load.

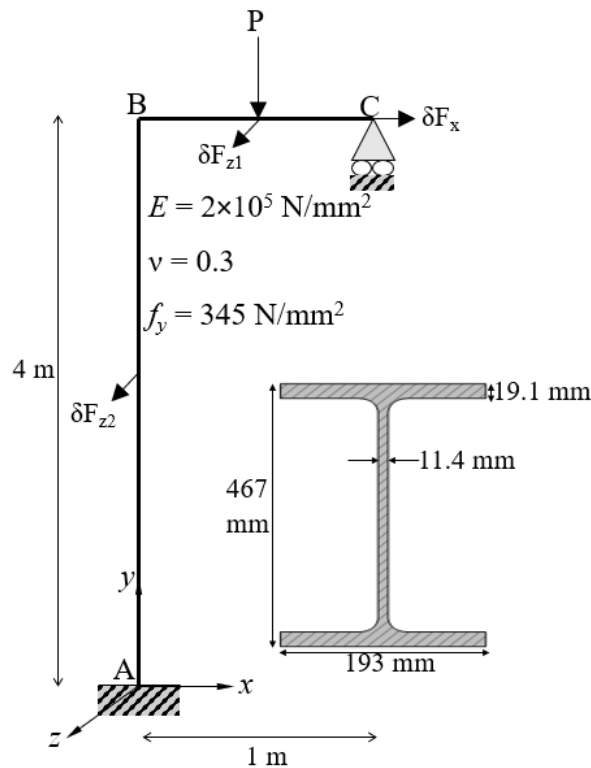


Figure 6: Cantilever right-angled frame

Figure 6 shows a right-angled cantilever frame with a beam subjected to in-plane gravity loads at the midspan of the beam, which primarily fails through lateral-torsional buckling of the beam. A, B, and C are restrained against out-of-plane sway deformations. δF_x , δF_{z1} , and δF_{z2} represent the fictitious lateral notional loads applied, to perturb the perfect frame in its primary path to the

desired secondary path. If a horizontal notional load alone ($\delta F_x \neq 0, \delta F_{z1} = 0, \delta F_{z2} = 0$) is applied, the out-of-plane deformations will be zero. To trigger the torsional mode, the notional load applied should be in the z-direction at the column midheight ($\delta F_x = 0, \delta F_{z1} = 0, \delta F_{z2} \neq 0$). The frame is adequately restrained from out-of-plane deformations at joints B and C. This reduces the effective length of the beam-column for the limit state of lateral-torsional buckling. The in-plane and out-of-plane deformed shapes of the frame are shown in Figure 7.

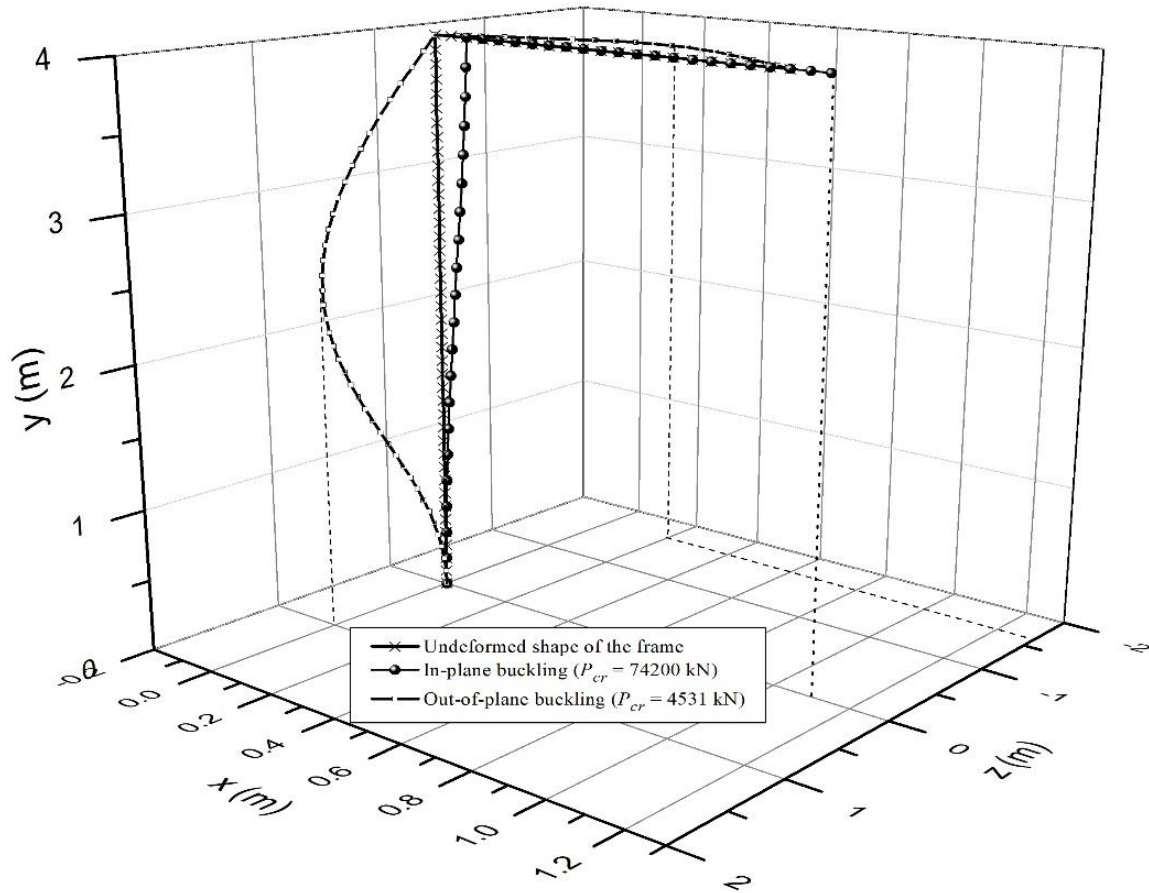


Figure 7: The deformation modes of the frame

Different combinations of notional loads were applied on the frame, and the P_u-M_u curves were plotted against the in-plane interaction curve for DAM. The attributes of each of the frame models used for ELM and DAM and the capacities predicted by each model are given in Table 2. Figure 8 shows the $P-M$ curves for models 1, 2, 3, and 4, along with the interaction curves for ELM ($K=1.2$) and DAM ($K=1$). For model 1, the P_u-M_{ux} curve represents the true response of the frame under applied loads. The effect of member imperfections and member inelasticity is included in the determination of P_n , and M_{nx} . The sway stiffness of the frame is too high when compared to the torsional stiffness of the frame. As a result, for the same level of applied load, significant deformations occur in the case of Model 4, when compared to Models 2 & 3. This results in a higher major axis moment demand on the beam-column for Model 4. The column is heavily loaded in uniaxial compression, hence DAM predicts a higher load-carrying capacity for the beam-column than ELM, when the notional loads are placed at B and C. Applying an out-of-plane

notional load at A results in a more accurate model for DAM, predicting the load carrying capacities in agreement with ELM.

Table 2: Modeling parameters for analysis of cantilever frame in Figure 6

| | Parameter | ELM | DAM | | |
|-------------------------------------|---|--|--|--|--|
| | | Model 1 | Model 2 | Model 3 | Model 4 |
| Modeling for nonlinear analysis | Stiffness reduction factor | 1 | 0.8 | 0.8 | 0.8 |
| | Notional loads | No ($\delta F_x=0$, $\delta F_{z1}=0$, $\delta F_{z2}=0$) | One in-plane notional load ($\delta F_x=1$ kN, $\delta F_{z1}=0$, $\delta F_{z2}=0$) | One out-of-plane notional load ($\delta F_x=0$, $\delta F_{z1}=1$ kN, $\delta F_{z2}=0$) | One out-of-plane notional load ($\delta F_x=0$, $\delta F_{z1}=1$ kN, $\delta F_{z2}=0$) |
| Determination of P_n and M_n | Effective length factor (K) | 1.2 | 1 | 1 | 1 |
| | Nominal compressive strength, P_n (kN) | 1954.7 | 2257.4 | 2257.4 | 2257.4 |
| | Member major axis flexural strength, M_{nx} (kNm) | 683.8 | 683.8 | 683.8 | 683.8 |
| Determination of P_u and M_{ux} | Allowable compressive force, P_u (kN) | 1718.3 | 1992.4 | 1992.6 | 1516.5 |
| | Allowable major axis moment, M_{ux} (kNm) | 7.82 | 9.11 | 9.35 | 101.9 |

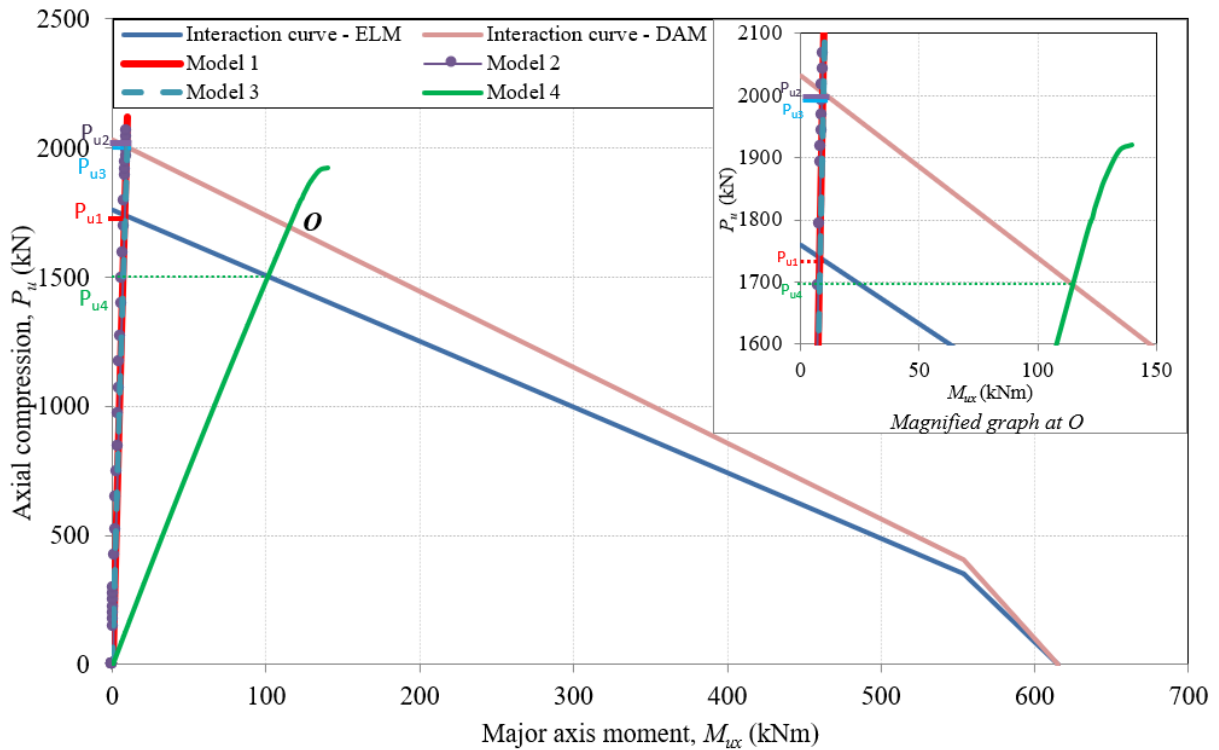


Figure 8: In-plane interaction curves for ELM and DAM

4. Conclusions

Using an exact 3D TL second-order analysis formulation, benchmark problems for DAM are proposed in this paper. The main contribution of the paper is to demonstrate that without a proper set of notional loads, it is likely that the governing design demand may be missed. Two benchmark problems are presented to demonstrate that the flexural-torsional limit state, which if ignored, might result in unsafe design using DAM. It also discusses the concept of notional loads as per ANSI/AISC–360-16. A planar frame with in-plane gravity loading and major axis flexure, when subjected to geometric nonlinear effects undergoes flexure-only deformations corresponding to the sway mode. When the frame has torsionally flexible cross-sections, then a small out-of-plane perturbation itself will drive to a flexural-torsional post-buckled state, exhibiting very large deformations (in-plane and out-of-plane). The necessity of modeling the spatial deformation of the frame on the accuracy of DAM is demonstrated in this paper. When the frame is adequately restrained against out-of-plane sway deformations, the minor axis flexure demand is nominal. Yet different combinations of notional loads result in varied predictions of the ultimate capacity. In this case, the notional loads were applied as inter-member loads instead of nodal loads. It is suggested that even when the topology of the frame does not highlight the need for a 3D analysis, a designer intending to use DAM have to try a few combinations of in-plane and out-of-plane notional loads to correctly assess the entire spectrum of deformation responses of the frame if the behavior of the structure is not completely understood by the designer.

References

- ANSI/AISC 360. 2016. *Specification for Structural Steel Buildings*.
- Chen, W. F., and S. Toma. 1994. *Advanced analysis of steel Frames*.
- Dierlein G. 2003. *Background and Illustrative Examples on Proposed Direct Analysis Method for Stability Design of Moment Frames*.
- Du, Z. L., Z. X. Ding, Y. P. Liu, and S. L. Chan. 2019. “Advanced flexibility-based beam-column element allowing for shear deformation and initial imperfection for direct analysis.” *Eng Struct*, 199. Elsevier Ltd.
- Ingkiriwang, Y. G., and H. Far. 2018. “Numerical investigation of the design of single-span steel portal frames using the effective length and direct analysis methods.” *Steel Construction*, 11 (3): 184–191. Ernst und Sohn.
- Pai, P. F. 2007. *Highly Flexible Structures: Modeling, Computation, and Experimentation*. *Highly Flexible Structures: Modeling, Computation, and Experimentation*. American Institute of Aeronautics and Astronautics.
- Pai, P. F. 2011. “Geometrically exact beam theory without Euler angles.” *Int J Solids Struct*, 48 (21): 3075–3090.
- Pai, P. F. 2014. “Problems in geometrically exact modeling of highly flexible beams.” *Thin-Walled Structures*, 76: 65–76.
- Pai, P. F., T. J. Anderson, and E. A. Wheeler. 2000. “Large-deformation tests and total-Lagrangian finite-element analyses of flexible beams.” *Int J Solids Struct*.
- Shankar Nair, R., and R. S. Nair. 2007. *Stability Analysis and the 2005 AISC Specification NASCC: THE STEEL CONFERENCE. MODERN STEEL CONSTRUCTION*.
- Surovek, A. E., and R. D. Ziemian. 2005. “The direct analysis method: Bridging the gap from linear elastic analysis to advanced analysis in steel frame design.” *Proceedings of the Structures Congress and Exposition*, 1197–1210.
- Surovek, A., and D. W. White. 2001. *Direct Analysis Approach for the Assessment of Frame Stability: Verification Studies Engineering Creativity View project Direct Analysis and Steel Frame Stability View project*.
- Teh, L. H. 2004. “Beam element verification for 3D elastic steel frame analysis.” *Comput Struct*, 82 (15–16): 1167–1179.
- Ziemian, C. W., and R. D. Ziemian. 2021a. “Efficient geometric nonlinear elastic analysis for design of steel structures: Benchmark studies.” *J Constr Steel Res*, 186. Elsevier Ltd.
- Ziemian, C. W., and R. D. Ziemian. 2021b. “Steel benchmark frames for structural analysis and validation studies: Finite element models and numerical simulation data.” *Data Brief*, 39. Elsevier Inc.
- Ziemian, R. D., and J. C. B. Abreu. 2018. “Design by advanced analysis – 3D benchmark problems: Members subjected to major- and minor-axis flexure.” *Steel Construction*, 11 (1): 24–29. Wiley-Blackwell.
- Ziemian, R. D., J. C. Batista Abreu, M. D. Denavit, and T.-J. L. Denavit. 2018. “Three-Dimensional Benchmark Problems for Design by Advanced Analysis: Impact of Twist.” *Journal of Structural Engineering*, 144 (12). American Society of Civil Engineers (ASCE).